XVI International Conference on Durability of Building Materials and Components
DBMC 2023, China
K.F. Li and D.P. Fang (Eds)

Effectiveness of Paraffin-based Curing Compound for Mitigation of the Plastic Shrinkage and Related Cracking of the 3D-printed Concrete Elements

Slava Markin, Viktor Mechtcherine

TU Dresden, Institute of Construction Materials, Dresden, Germany

slava.markin@tu-dresden.de, viktor.mechtcherine@tu-dresden.de (Corresponding author)

Abstract. *3D-printed concrete elements are highly vulnerable to early-age shrinkage and cracking compared to conventionally cast concrete elements. Material compositions of printable concretes and complete renunciation of shuttering are responsible for accelerated capillary pressure build-up, leading to volumetric constructions of the 3D-printed layers at a very early age after extrusion and enhanced shrinkage at a later age. Shrinkage-induced cracks can severely impair the durability and appearance of 3D-printed concrete structures. The study at hand analyses the efficacy of the paraffin-based curing agent for reducing the shrinkage and cracking of 3D-printed elements and structures. Development of the temperature and capillary pressure, as well as shrinkage strains, were reported for the cured and uncured specimens. The study results show that applying paraffin-based curing agents can considerably reduce shrinkage-indued deformations of the 3D-printed elements produced even under extreme environmental conditions.*

Keywords: *Plastic shrinkage; Plastic shrinkage cracking; Capillary pressure; 3D-printing; Durability*

1 Introduction

3D concrete printing (3DCP) has evolved in recent years from an audacious idea to a promising building technique. Produced worldwide 3D-printed residential buildings and infrastructural objects demonstrated the viability of the new technology (Bos et al. 2022). Unfortunately, the durability and serviceability of printed objects are greatly diminished by the high shrinkage and related cracking (Markin and Mechtcherine 2023). The printable compositions' specific material properties and the production technique's particularities make them highly vulnerable to plastic, drying and autogenous shrinkage. The classification of the shrinkage types and the mechanism behind them are detailed in (Srinivas 2014).

Among various techniques for mitigating shrinkage and related cracking, adding fibres and applying curing agents appears to be the most promising (Hajibabaee et al. 2018). Curing agents could be applied right after the extrusion of the concrete layers by spraying them on the concrete's surface. The curing agent forms a film which prohibits evaporation. 3D-printed elements suffer even more than conventionally cast concrete elements from rapid evaporation of the pore water. Therefore, reducing the water evaporation accomplished by optimising the composition of printable concretes is essential for the mitigation of shrinkage-induced deformations. Sealing the surfaces of 3D-printed elements with curing agents may reduce early-age shrinkage, i.e., plastic shrinkage, and also beneficially affect the later types of shrinkage, such as drying and autogenous shrinkage.

The study at hand focuses on analysing the efficacy of the paraffin-based curing agent for

reducing the shrinkage of 3D-printed concrete elements. The evolution of the concrete temperature and capillary pressure is measured on the 3D-printed concrete wall with and without the application of the curing agent. Moreover, deformations of the cured and uncured walls are measured with a 3D-digital image correlation system. Analysis of the shrinkage-induced strains is limited to longitudinal deformations.

2 Materials and methods

A detailed description of the reference mixture used in this study is provided in (Markin and Mechtcherine 2022). For the investigation, 240 litres of reference compositions were produced by a four-time repeated mixing of 60 litres. Produced batches were intermixed and transported to the 3D-printing test device (3DPTD) equipped with a rectangular nozzle with an opening of 150 mm x 50 mm, detailed in (Mechtcherine et al. 2019). The specimen was printed on the stainless steel printing table of the 3DPTD. No release agents or other substances were applied to the printing table. The moving speed of the printhead was set to 40 mm/s. The layer-to-layer deposition time interval (TI) was 2 min. The experiment's ambient temperature and relative humidity were 20±1°C and 60±5%. Figure 1 depicts the extrusion process. The length of the produced wall was approx. 155 cm.

Figure 1. 3D-printed concrete wall.

A relatively small TI between the deposition of the layers and the high self-weight of the layers induced the deformation of the bottom layers, see Figure 2. Right after extrusion 3D-printed wall was divided with the steel wire into two specimens. The left specimen served as a reference and was left untreated. To the right specimen was applied paraffin-based curing agent (MasterKurve 216WB, BASF Construction Solutions GmbH, Straßfurt, Germany) by spraying it with a manually operated sprayer. The application rate by manual spraying of the curing compound was approx. 150 g/m². After that, specimens were prepared for the contactless measurement of the deformations with a 3D-digital image correlation system (ARAMIS Adjustable, Carl Zeiss GOM Metrology GmbH, Braunschweig, Deutschland). Measuring markers of a diameter of 5.0 mm were glued to the steel nails and then introduced to each layer at the respective places. To the middle of two upper layers were introduced tensiometers to a depth of approx. 7.0 cm. Temperature gauges were introduced to the same layers below the tensiometers. The ambient conditions, including temperature and relative humidity, were

recorded with Lascar Electronics EL-USB-1-LCD Datalogger (Lascar Electronics, Whiteparish, UK). Measuring of the material properties and deformations was started simultaneously after 170 min from the time of water addition (TWA). The experiment lasted 24 hours.

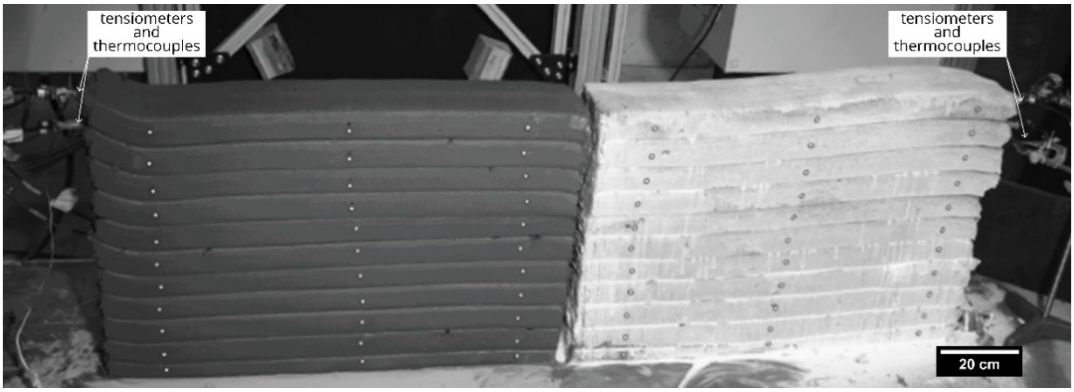

Figure 2. (a) Uncured reference 3D-printed specimen, (b) Cured with MK216 3D-printed specimen.

3 Results and discussion

3.1 Evolution of the temperature and capillary pressure

Figure 3 shows the evolution of the capillary pressure in the cured and uncured specimens. In the uncured specimen, capillary pressure starts to build up much earlier than in the cured specimen.

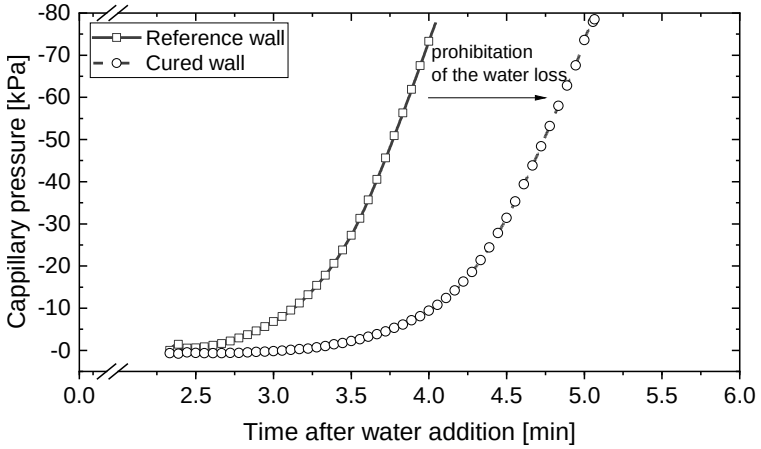

Figure 3. Evolution of the capillary pressure in the cured and uncured specimen.

Application of the curing compound prohibited evaporation and consequently retarded the beginning of the capillary pressure growth for approx. 1.1 hours. Retardation of the evolution of capillary pressure is essential for mitigating shrinkage-induced deformations. In this way, the material has time to gain enough strength to resist contractional forces in capillaries. Under the assumption that the evaporation of the cured specimen is completely prohibited, the evolution of capillary pressure was driven only by self-desiccation due to progressing hydration. Even more, it could be assumed that the development of capillary pressure in the cured

specimen started when the specimen was already transmitted to the solid state, which diminished the effect of negative capillary pressure on the shrinkage of the specimen.

The temperature of the uncured and cured specimens begins to rise rapidly approximately 4 hours after TWA, see Figure 4. Worth to note that cured specimen experiences a much higher temperature than the uncured specimen. This could be explained by the isolating effect of the sealing film provided by the curing agent. Additionally, the uncured specimen was able to emit the inner temperature due to the effect of the evaporative cooling. Note that the beginning of the evolution of the capillary pressure in the cured specimen corresponds to the start of temperature growth, which confirms the effect of hydration on the evolution of capillary pressure.

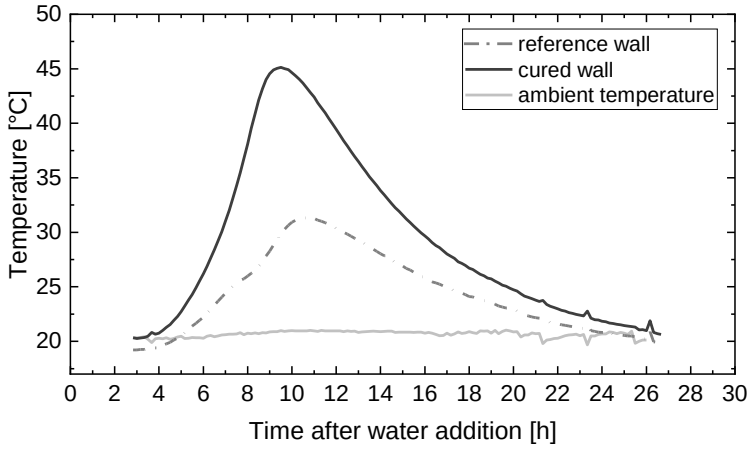

Figure 4. Ambient temperature and the evolution of the concrete temperature.

3.2 Horizontal shrinkage

Figure 5a shows the horizontal shrinkage of the layers of the reference specimen in a longitudinal direction. The top layers shrink significantly more than the bottom layers. Such deformation behaviour was found to be typical for 3D-printed elements (Markin and Mechtcherine 2023). The bottom layers experience more restriction due to the interaction with the printing table and the hydrostatic pressure from the overhead layers. Note that the top layers possess higher water content due to later exposure to desiccation than the bottom layers. However, the top layer of the printed specimen is exposed from three planes to desiccation, which leads to a higher evaporation rate and, consequently, higher shrinkage. Inherently, high shrinkage of the top layer and later shortage of disposed of "free water" for evaporation enhance shrinkage of the underlying layers. Moreover, there is a remarkable phenomenon of deformations reversing direction after 4 hours after TWA and shrinking again after 8 hours.

In contrast to the uncured specimen, deformations of the layers of the cured specimen are more consistent, i.e., there is no significant difference in shrinkage of the top and bottom layers, see Figure 5b. Interestingly, contrary to the uncured specimen, the layers of cured specimen right after the beginning of the experiment experience extension. Only after approx. 8 hours from the TWA, shrinkage becomes more pronounced. Section 3.3 discusses in detail how this phenomenon is related to the evolution of temperature in the specimens. Worth noting that after approx. 24 hours after TWA cured specimen shows more than three times less shrinkage than

the uncured specimen.

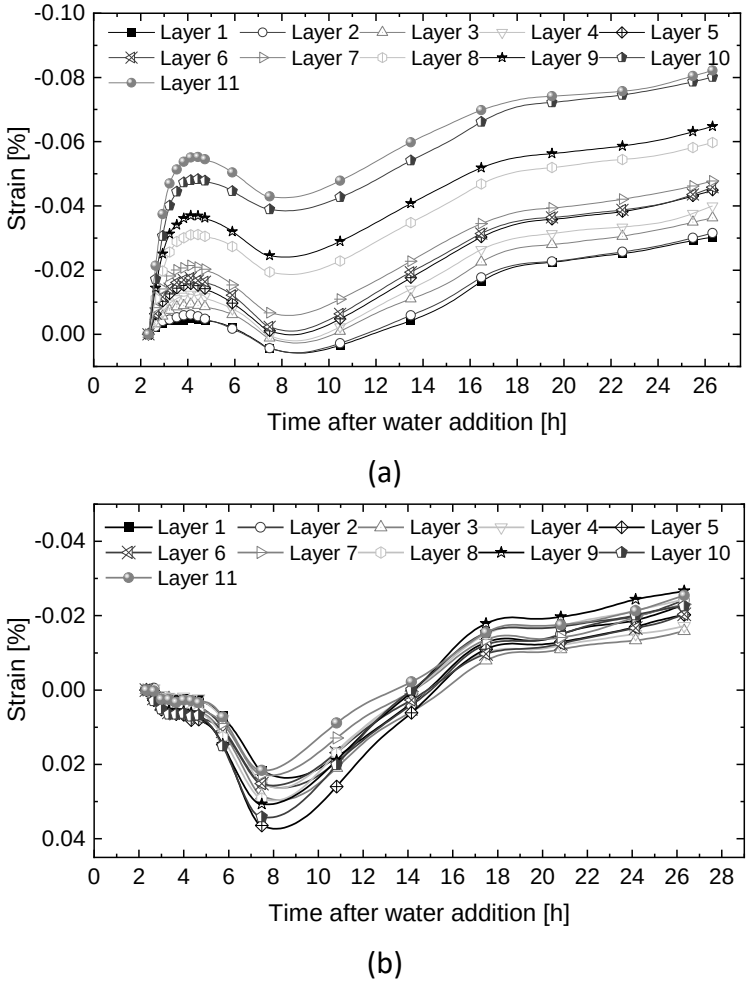

Figure 5. (a) Horizontal shrinkage of the uncured 3D-printed wall, (b) Horizontal shrinkage of the cured 3D-printed wall.

3.3 The effect of thermal expansion

Due to the release of hydration heat, temperature evolution greatly affects the deformation behaviour of the 3D-printed elements. Figure 6a visualises the effect of thermal expansion on the deformation behaviour of the uncured specimen. As expected, right after the beginning of the experiment 3D-printed specimen undergoes shrinkage, depicted in Figure 6 with 1. As temperature increases, thermal expansion dominates the shrinkage, depicted with 2. Most likely, phase 2 is already related to the deformations of the specimen in a solid state. It could be assumed that transmission from plastic state to solid happens approx. at 4 hours after TWA, and starting from that time, all shrinkage-induced deformations are related to autogenous and drying shrinkage. The specimen shrinks again once the pick of hydration reaction is overcome and the temperature begins to decrease, depicted with 3. The top and bottom layers of the specimen experience equal deformation behaviour. The bottom layer, however, has a lower deformation rate than the top layer. Approx. after 18 hours after TWA the rate of deformations

decelerates, which is most probably attributed to the slow-down of the hydration reaction.

In the cured specimen, capillary pressure does not play a dominant role in the deformation behaviour due to the prohibition of evaporation. Even more, right after the beginning of the experiment, cured specimen experience extension, see phase 1 in Figure 6b. As the temperature rises, the rate of extension increases as well, depicted with 2. The pick of extension is reached when the specimen's temperature riches its maximum of 45°C. After that, similar to the uncured specimen, the temperature starts to decrease, and the shrinkage begins to dominate the thermal extension, depicted with 3. Declaration of the deformations, as depicted with 4, most probably indicates the retardation of the hydration process.

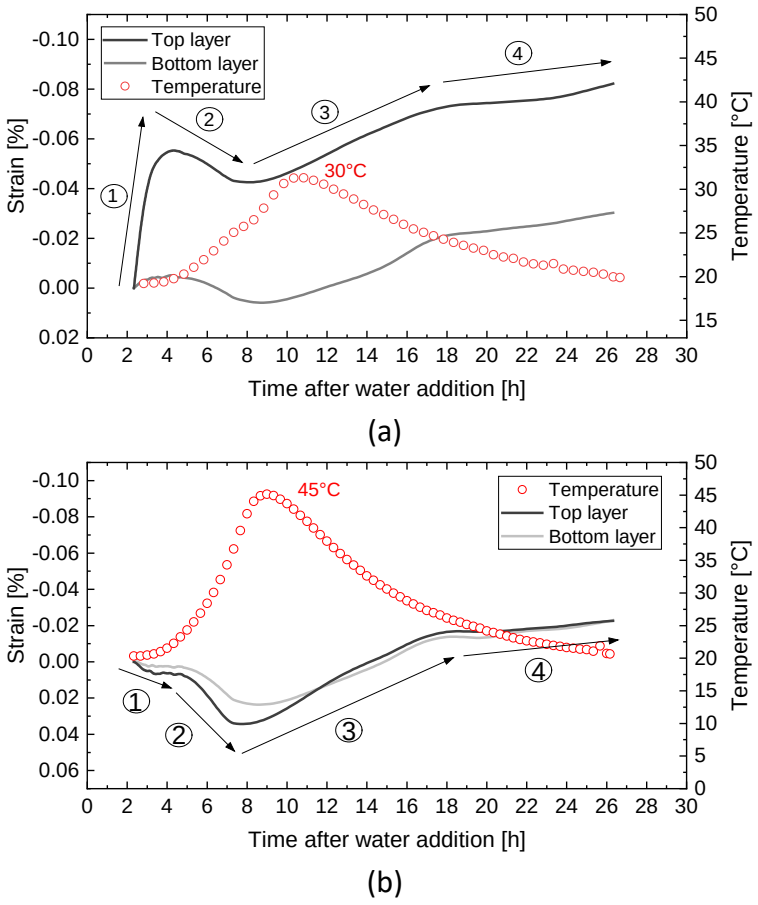

Figure 6. The effect of the thermal expansion on the shrinkage-induced deformations: (a) uncured 3D-printed wall, (b) cured 3D-printed wall.

4 Conclusions

The article at hand presented a simple and effective method for the reduction of the shrinkage-induced deformations of the 3D-printed concrete elements. A 3D-printed wall cured with a paraffin-based agent showed up to three times less horizontal shrinkage strain than an uncured reference wall. Additionally, it was found that 3D-printed concrete elements may experience significant thermal expansion, which contracts shrinkage-induced deformations. The analysis of the vertical deformations was not included in the current article and will be presented in

future authors' publications. Among the topics that should be covered in future studies on the effectiveness of paraffin-based curing agents for mitigation of shrinkage-induced deformations and cracking of the 3D-printed concrete elements are:

- Modification of the composition of the binder and its effect on shrinkage by applying paraffin-based curing agents.
- The effect of thermal expansion on the interlayer bond strength.
- Combination of the paraffin-based curing agents with passive mitigation approaches for reduction of shrinkage-induced deformations.
- Automation of the inline curing of the 3D-printed walls.
- The effect of treatment with paraffin-based curing compounds on post-processing of the 3D-printed elements such as, e.g. plastering or colouring.
- Effectiveness of the paraffin-based curing compounds under extreme environmental conditions.

Acknowledgements

This work is a portion of S. Markin's PhD research and a part of the project funded by the Deutsche Forschungsgemeinschaft (DFG, German Research Foundation), Project Number 424803818.

ORCID

Slava Markin: http://orcid.org/0000-0001-8874-0078
Viktor Mechtcherine: http://orcid.org/0000-0002-4685-7064

References

Bos, F. P., Menna, C., Pradena, M., Kreiger, E., da Silva, W. LealR., Rehman, A. U. et al. (2022): *The realities of additively manufactured concrete structures in practice.* In Cement and Concrete Research 156, p. 106746. DOI: 10.1016/j.cemconres.2022.106746.

Hajibabaee, A., Khanzadeh M. M., Ley, M. T. (2018): *Comparison of curing compounds to reduce volume change from differential drying in concrete pavement.* In International Journal of Pavement Engineering 19 (9), pp. 815–824. DOI: 10.1080/10298436.2016.1210442.

Markin, S., Mechtcherine, V. (2022): *Measuring Plastic Shrinkage and Related Cracking of 3D Printed Concretes*. In: Third RILEM International Conference on Concrete and Digital Fabrication. Digital Concrete 2022, vol. 37. 1st ed. 2022. Cham: Springer International Publishing; Imprint Springer (Springer eBook Collection, 37), pp. 446–452

Markin, S., Mechtcherine, V. (2023): *Quantification of plastic shrinkage and plastic shrinkage cracking of the 3D printable concretes using 2D digital image correlation.* In Cement and Concrete Composites, p. 105050. DOI: 10.1016/j.cemconcomp.2023.105050

Mechtcherine, V., Nerella, V. N., Will, F., Näther, M., Otto, J., Krause, M. (2019): *Large-scale digital concrete construction – CONPrint3D concept for on-site, monolithic 3D-printing.* In Automation in Construction 107, p. 102933. DOI: 10.1016/j.autcon.2019.102933.

Srinivas, A. (2011): *State-of-the-Art Review on Early-Age Shrinkage of Concrete.* In Indian Concrete Journal 85 (7), pp. 14-20